Proceedings 10th NUMGE 2023
10th European Conference on Numerical Methods in Geotechnical Engineering
Zdravkovic L, Kontoe S, Taborda DMG, Tsiampousi A (eds)

https://doi.org/10.53243/NUMGE2023-251

Flow liquefaction and large deformation analysis in a tailings dam using MPM and critical state-based material modelling

E. Lino Ramírez[1,2], M. Taiebat[1], A. Lizcano[2]

[1]*Department of Civil Engineering, University of British Columbia, Vancouver, Canada*
[2]*SRK Consulting, Vancouver, Canada*

ABSTRACT: This study explores the capabilities of the Material Point Method (MPM) and a critical state-compatible, bounding surface plasticity model for sands to simulate the flow liquefaction phenomenon and the subsequent runout distance following a tailings dam failure. A boundary value problem, inspired by a real failure of an upstream tailings dam, was simulated using MPM and the computational platform Anura3D. The SANISAND constitutive model is used to simulate the response of the tailings, and its parameters are calibrated using undrained triaxial test results. An increase in pore pressure was imposed in the foundation as the triggering event. The results highlight the capabilities of the MPM and SANISAND in simulating the complex mechanisms involved in tailings dam failures and provide insights into flow liquefaction material behaviour during such events.

Keywords: MPM; SANISAND; large deformations; flow liquefaction; tailings

1 INTRODUCTION

Over the past few years, there have been several devastating failures of tailings dams, resulting in severe human and environmental consequences (e.g., Morgenstern et al., 2016, Robertson et al., 2019). The recent spate of tailings dam failures has been primarily attributed to the flow liquefaction of loose, saturated tailings, often triggered by static loading conditions. This has increased the need for advanced numerical simulations that go beyond the limitations of classical limit equilibrium analysis typically used in engineering practice, to better understand the risks associated with tailings dam failures and the extent of the tailings runout. Numerical simulations of tailings dam failures and runout necessitate a constitutive model that can accurately capture the undrained response of loose, saturated tailings, and a computational platform that can efficiently handle the large deformations involved in such catastrophic events.

This study investigates the efficacy of using a critical state bounding surface plasticity model for sand and the Material Point Method (MPM) computational technique to simulate the flow liquefaction of tailings and the resulting extent of runout after a tailings dam failure. The study simulates a boundary value problem inspired by a real-life failure (Davies et al., 1998) of a 12-meter-high upstream dam constructed on loose, saturated tailings. Specifically, the study aims to assess the ability of the MPM and critical state-based material modelling to more accurately capture the complex behaviours and large deformations involved in such catastrophic events.

The simulation was carried out using the Anura3D platform (Anura3D, 2021) with the SANISAND constitutive model. The constitutive parameters of the model were calibrated based on undrained triaxial tests of polymetallic tailings. The SANISAND constitutive model was shown to capture the contractive brittle behaviour of saturated loose tailings observed in laboratory data. The simulation of the deformation process utilized the two-phase single-point MPM formulation, with the foundation's increase in pore water pressure being the trigger for failure initiation. To the authors' knowledge, this is the first application of the SANISAND constitutive model to study large deformations problems in the MPM framework.

The use of numerical simulations is critical for gaining insights into flow liquefaction onset, subsequent large deformations, and material behaviour during large deformation. This study emphasizes the significance of utilizing advanced numerical models and simulations in tailings dam design and management to prevent or mitigate the consequences of tailings dam failures.

2 CONSTITUTIVE MODEL

The phenomenon of flow liquefaction of loose, saturated clean sands and tailings resulting from static loading (static liquefaction) has been widely documented in the geotechnical literature (Castro, 1969; Ishihara, 1993; Leong et al., 2000; Schnaid et al., 2013; Riveros and Sadrekarimi, 2021; Macedo and Vergaray, 2022). The constitutive model used in the present study follows the basic premises of the original two-surface plasticity model of Manzari and Dafalias (1997) and revised by Dafalias and Manzari (2004), which formed the basis of what Taiebat and Dafalias (2008) later on named SANISAND class of models. The SANISAND models are formulated based on the principles of critical state soil mechanics (CSSM) and bounding surface plasticity. The Dafalias and Manzari (2004) that is referred to as SANISAND in this paper, represents the core of the constitutive model, and various subsequent works include the extensions of the SANISAND class (e.g., Dafalias and Taiebat 2016, Petalas et al. 2020, Barrero et al. 2020, and Yang et al. 2022).

Despite its usefulness in simulating natural granular materials such as clean sand, the SANISAND model has not, to the best of the authors' knowledge, been applied to tailings simulation. No published SANISAND constitutive parameters specifically for tailings were found in the technical literature. This study aims to establish the model parameters for a particular polymetallic tailings material, which consists of a non-plastic sandy material with a fines content of 75% (see Fig. 1).

The calibration process was based on the method presented by Taiebat et al. (2010). From the conducted triaxial tests, a subset of three undrained triaxial tests with confining pressures of 48, 75, and 300 kPa, and corresponding void ratios of 0.603, 0.774, and 0.684, respectively, were selected for calibration purposes. The results of the triaxial tests were used to derive the critical state parameters for the model. The model parameters, which were obtained from the calibration process, are listed in Table 1. Additional information on the calibration process can be found in Lino (2021).

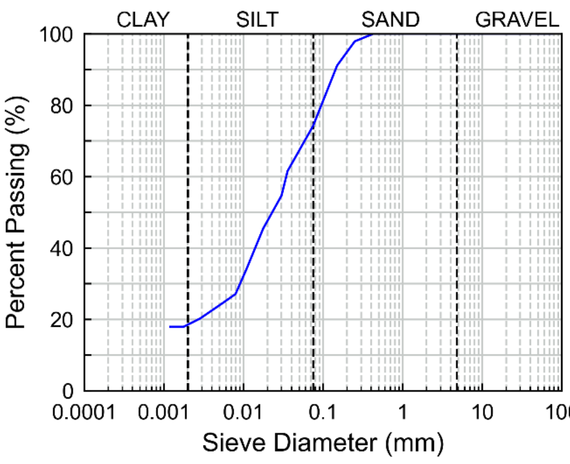

Figure 1. Particle Size Distribution of polymetallic tailings

The comparison between the laboratory results and the undrained triaxial simulations using SANISAND and the parameters in Table 1 is presented in Fig. 2. The comparison demonstrates the ability of SANISAND to accurately simulate the flow liquefaction behaviour under monotonic loading observed in the laboratory, making it a valuable tool for predicting the behaviour of loose, saturated tailings.

Table 1. Material parameters of the SANISAND model for polymetallic tailings

Parameter	Symbol	Value	Parameter	Symbol	Value
Elasticity	G_0	125	Dilatancy	n^d	1.1
	ν	0.05		A_0	0.2
Critical state	M_c	1.5	Kinematic hardening	n^b	1.1
	c	0.712		h_0	7.05
	e_c	1.191		c_h	1.1
	λ_c	0.545	Fabric dilatancy	z_{max}	4.0
	ξ	0.14		c_z	600

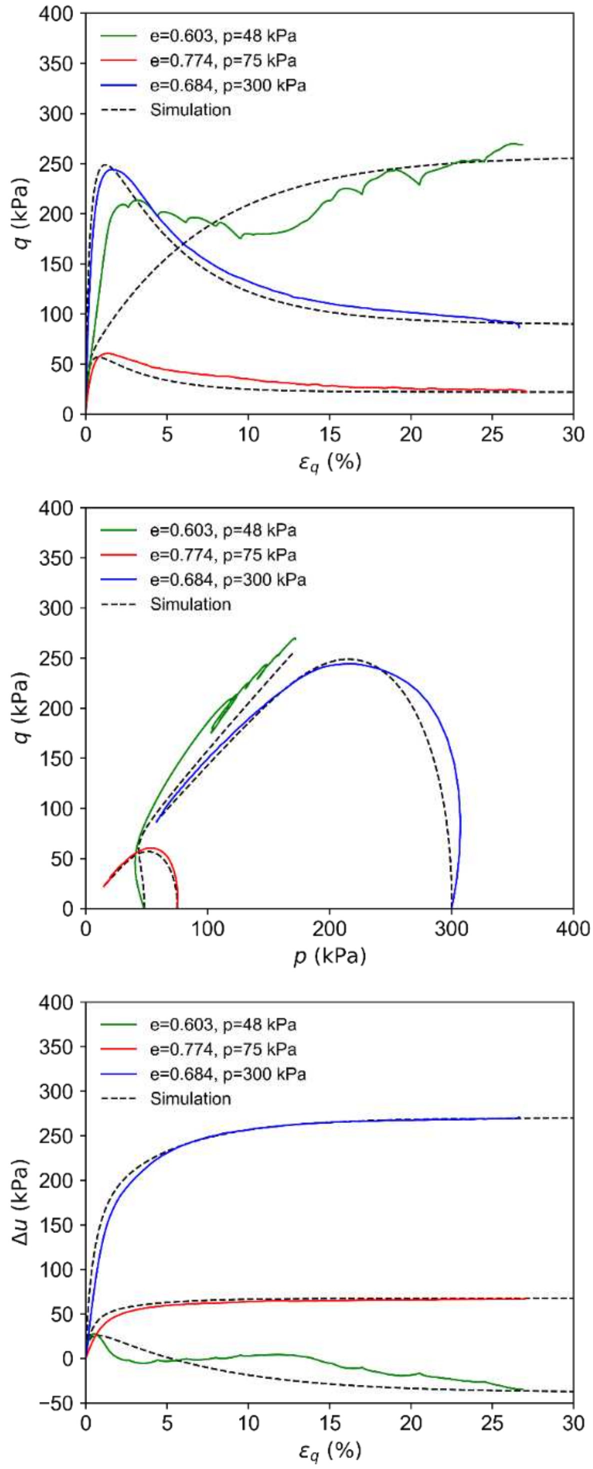

Figure 2. Performance of the calibrated model in simulation of undrained triaxial tests on polymetallic tailings

3 SIMULATION OF A TAILINGS DAM FAILURE

The boundary value problem investigated in this study was motivated by the historical failure of a dam resulting from the liquefaction of tailings, as documented in Davies et al. (1998). However, it should be noted that the tailings material analyzed in our study is not the same as that involved in the aforementioned event. Rather, we focused on a polymetallic tailings material described in the previous section, to showcase the capabilities of advanced constitutive modeling along with the MPM technique in simulating the state evolution of material and the associated large deformation process when subjected to a failure trigger.

3.1 Geometry and sequence of modelling

Figure 3 presents the 2D model, which is 130 m wide and includes a main dam that is 12 m high and constructed from compacted tailings with 1.4:1 upstream and downstream slopes. The main dam is reinforced by a 6.5 m high waste rock buttress, with a crest width of 5 m and a 4:1 slope. The starter dam and the 8 m thick dense impounded tailings (upper tailings) rest on top of the 7 m thick historical loose saturated tailings (lower tailings). The historical tailings are contained by an additional dam, built of the same material as the main dam, located 60m downstream from the main dam's toe. For MPM analysis, an unstructured mesh composed of triangular elements was developed, and refinements were added in zones susceptible to liquefaction. The mesh has an average element size of 1.5 m outside the lower tailings and 1.25 m inside, and it contains 3079 elements and 1652 nodes, with each element assigned three initial material points. Furthermore, the mesh was extended beyond the main dam to encompass the potential material point movements following failure.

Three simulation stages were executed. The initial effective stress and pore water pressure were calculated in stage 1, using a preliminary quasi-static simulation and the Mohr-Coulomb model. In stage 2, the SANISAND model was used for the tailings layers, and equilibrium was verified with another quasi-static simulation. In stage 3, the triggering event was applied to initiate the deformation process.

3.2 Triggering event

A triggering event is an action that leads to significant permanent deformations and destabilizes the tailings dam. It may involve a momentary or gradual change in loading conditions. The triggering event in this study is an increase in the pore water pressure at the base of the model, which represents an artificial recharge of water into the system. This is a common reason for causing slope instabilities and has been successfully used in simulations of the Selborne experiment (Soga et al., 2016) and flow slide flume tests (Cuomo et al., 2019). In both cases, the pore water pressure was applied to one boundary of the model. The pore water pressure at the base of the model was gradually increased over time, starting from 150 kPa at t=0 sec and increasing linearly to 200 kPa within 1 second. The authors acknowledge the limitations inherent in the employed trigger application method. Despite the simplifying assumptions incorporated in the numerical trigger implementation, the primary objective of this study is to initiate flow liquefaction in the lower tailings deposit and to provide a comprehensive evaluation of the pre- and post-failure behaviour of the tailings dam, as shown in Fig. 3.

3.3 Governing equations and method of solving

The MPM formulation incorporates the governing equations of a two-phase system, where the v-w approximation is utilized to describe the velocities of the solid and fluid phases (denoted by v and w, respectively) at a single point. The formulation also includes the interaction between the phases, which accounts for the dragging forces. The v-w approximation is described in greater detail in several references (Al-Kafaji, 2013; Ceccato, 2015; Yerro, 2015; Fern et al., 2019).

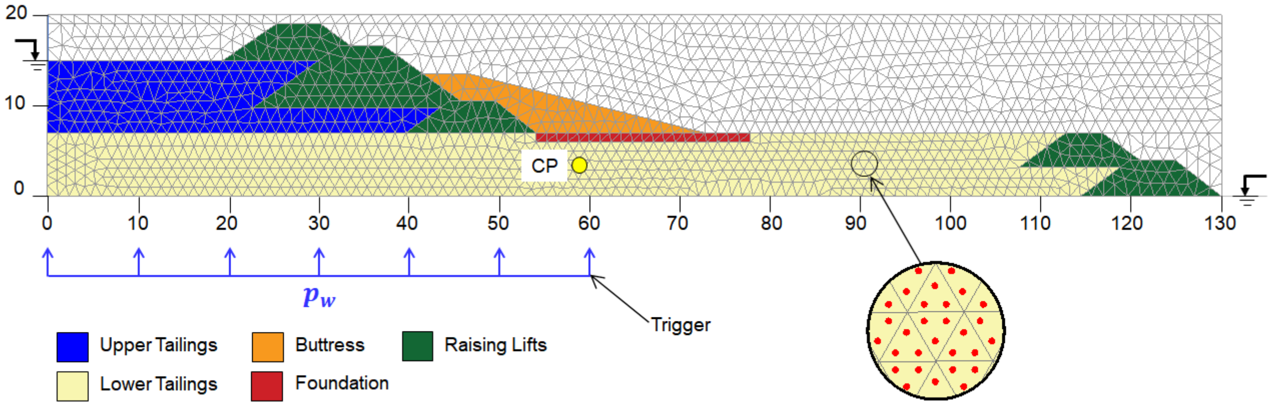

Figure 3. Tailings dam geometry, layering, water level, spatial discretization, MPM element, control material point (moving), and trigger applied: increment of pore water pressure

To stabilise the simulation, various settings were tested in Anura3D, including the software's strain smoothing option to minimize volumetric locking. This technique is based on the Nodal Mixed Discretization proposed by Detournay and Dzik (2006). Furthermore, increasing the number of material points was explored, but convergence issues were encountered. Notably, as highlighted by Fern and Soga (2016) and Kumar (2014), increasing the number of material points does not always improve the simulation results. Anura3D uses the MPM-mixed approach with a single Gauss point per element, which can result in non-convergence issues, especially when highly non-linear constitutive models such as SANISAND are employed or a large number of material points are present in the simulation.

Implemented in Anura3D, the v-w formulation successfully simulates saturated soil behaviour (Ceccato et al., 2016; Cuomo et al., 2019) by employing an explicit Euler-Cromer integration scheme to solve the discretized governing equations. The stability of this approach is dependent on the definition of the critical time step, which was set to 1E-4 for the simulations. In stages 1 and 2, a damping factor of 0.75 was utilized to attain an equilibrium state, while disregarding dynamic effects. In stage 3, a damping coefficient of 0.05 was used to reduce numerical instabilities.

3.4 Material models and parameters

In stage 1 of the simulation, the non-tailings (dam raises, foundation, and buttress) and tailings materials were modelled using an elastic-perfect plastic Mohr-Coulomb model with a non-associated flow rule, and with the parameters listed in Table 2. In stages 2 and 3, the SANISAND model was considered for the tailings, while the Mohr-Coulomb model was retained for the non-tailings materials. The SANISAND parameters were listed in Table 1. To account for the higher susceptibility of the lower layer to flow liquefaction, an initial void ratio of 0.82 was assumed for the lower layer, while the initial void ratio for the upper layer was assumed to be 0.75. The physical properties required for the analysis are listed in Table 3, which displays the parameters for all materials considered in the simulation.

Table 2. Adopted Mohr Coulomb parameters for non-tailings (raising lifts, foundation, and buttress) and tailings materials

Parameter	Symbol	Unit	Non Tailings	Tailings
Young's modulus	E	kPa	30,000	10,000
Poisson's ratio	v	-	0.3	0.3
Friction angle	ϕ	°	38, 36, 40*	36.9
Cohesion	c	kPa	1	0
Dilation angle	ψ	°	0	0

*Friction angles for the raising lifts, foundation, and buttress, respectively.

Table 3. Physical parameters for all materials used in the simulation

Parameter	Symbol	Unit	Value
Void ratio	e	-	0.75, 0.82, 0.50*
Solid density	ρ_s	kg/m^3	2700
Fluid density	ρ_f	kg/m^3	1000
Intrinsic permeability	k_f	m^2	1.0E-9
Bulk modulus fluid	K_f	kPa	2.15E4
Dynamic viscosity	μ_f	kPa/s	1.0E-6

*Initial void ratios for the upper tailings, lower tailings, and non-tailings materials, respectively.

3.5 Initial stresses and boundary conditions

Initial stresses were established by accounting for gravity, a K0 value of 0.5, and the void ratios and densities shown in Table 3. Both solid and fluid phases were subject to appropriate boundary conditions (BCs), including Essential and Natural BCs. Essential solid BCs were modelled as roller supports on the left and right sides of the model, while hinges at the bottom prevented vertical and horizontal displacements. At the top of the model, rollers restricted vertical displacement. Natural solid BCs dictated zero traction at the surface of the model. Essential fluid BCs were implemented at the left and right sides to limit horizontal movement. The top and bottom boundaries were considered impermeable, except for the location where pore water pressure (the triggering event) was imposed. Natural fluid BCs prescribed zero-water pressure at the model's surface.

4 RESULTS

This section provides a detailed description of the behaviour of tailings material during a tailings dam failure. Of particular interest is the response of the lower tailings, where a higher initial void ratio was assumed, and flow liquefaction is expected. Figure 3 shows the position of the material point CP within the lower tailings layer, which is used to assess the deformation process and stress path during the pre- and post-failure stages.

In Fig. 4, the evolution of deviatoric strains and mean effective stress is shown when an increment of pore water pressure is applied. The plot illustrates the initial and final configuration when equilibrium has been re-established, meaning when the velocity of the material points is equal to zero. The horizontal and vertical axes represent the dimensions of the model in meters. At t = 4 sec in Fig. 4a, there is a complete development of the shear surface within the tailings. As the tailings move, the thickness and extension of the shear zone increase. Fig. 4b shows that at t = 4 sec, the mean effective stress in the shear surface is reduced due to the application of the increment of pore water pressure. As the failure progresses, the mean pressures decrease, accelerating the deformation process of the system.

Figure 5 illustrates the performance of the tailings dam during the pre-failure, the onset of failure, and the subsequent motion when the triggering event is applied. In particular, this figure shows the behaviour of the tailings at the control point CP during the deformation process. The results provide a complete description of the pre-failure and subsequent motion when a critical state-based constitutive model is considered. The simulation results are presented using a sequence of time represented by points A, B, C, D, and E. At point A, which represents the beginning of the simulation at t = 0 sec, the mean effective stress reduces slightly due to the pore water pressure applied at the model's base. This reduction causes slight displacements of the control point CP without changes in the void ratio. At point B, which represents the onset of flow liquefaction, the mean effective stress starts to reduce dramatically, and the displacements suddenly increase. Between points B and C, a flow liquefaction behaviour is observed in the p-q plane, characterized by a significant loss of shear strength without warning. At point C, the material point reaches the critical state, and the tailings void ratio (e) and mean pressure (p) oscillate around the critical void ratio (e_c) and the critical mean pressure (p_c), respectively. Furtherefore, it should be noted that from C to D, the stress ratio (η) oscillates around the critical stress ratio (M_{CSL}), providing evidence that the tailings material reaches the critical state, and, therefore, large deformations are expected. At point D, the material point is about to stop and leave the critical state. Afterward, the pore pressure dissipates, and the mean pressure starts to increase until it reaches point E, which depicts the final condition at t = 16 sec. Overall, the results provide a comprehensive description of the pre-failure and subsequent motion, and they highlight the importance of considering the critical state-based sequence of response and flow liquefaction in lower tailings when analysing tailings dam failure.

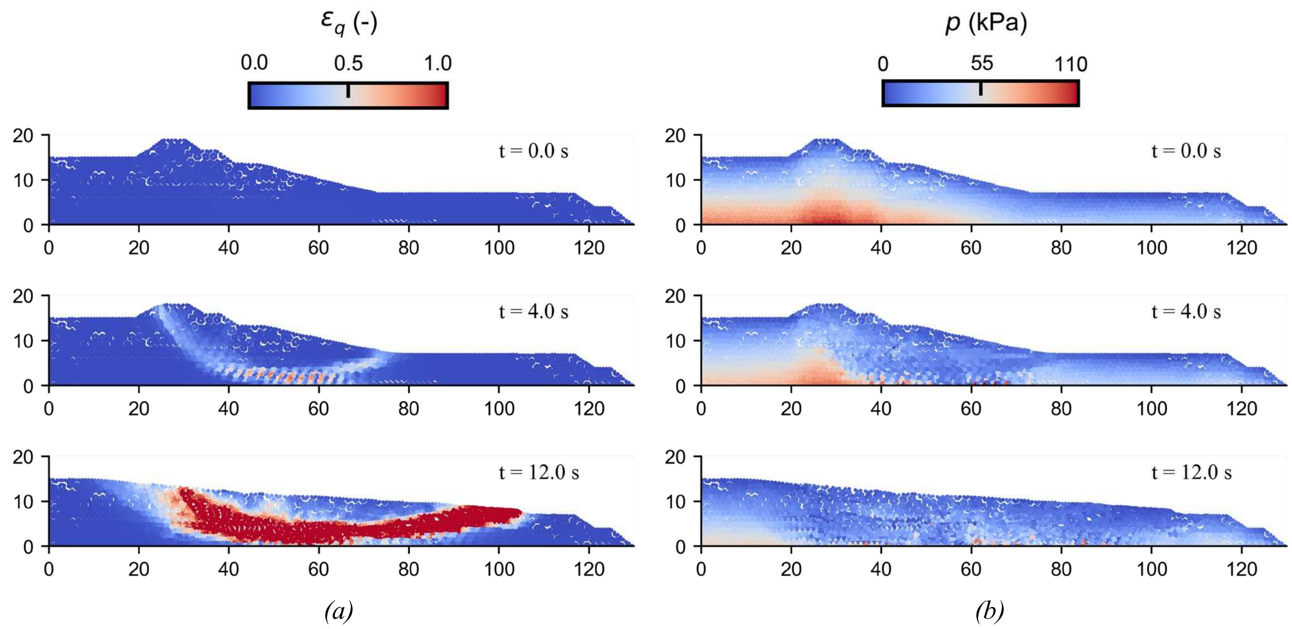

Figure 4. Evolution of deviatoric strains and mean effective stress during the deformation analysis

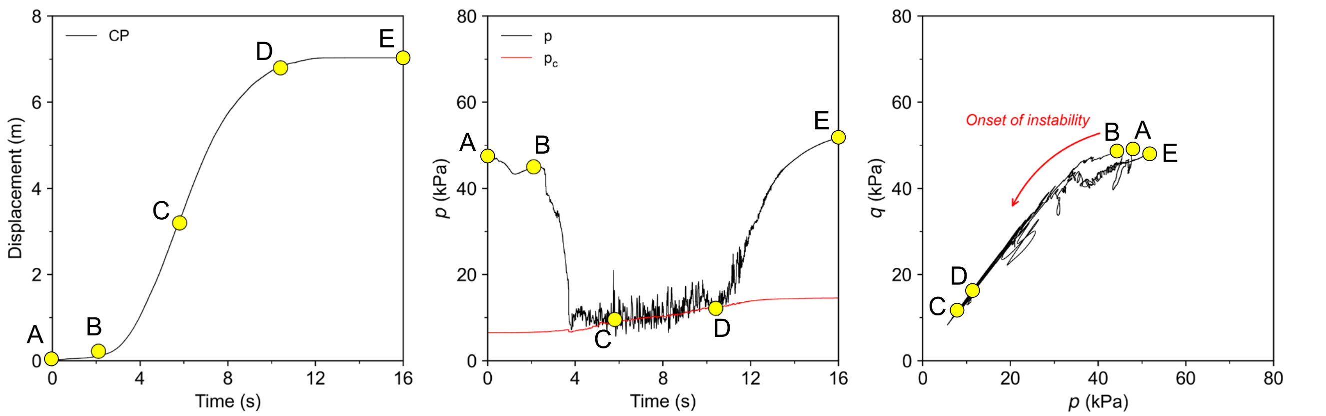

Figure 5. Evolution of the material state at control point CP (as shown in Figure 3) during the pre- and post-failure process

5 CONCLUSIONS

In this study, a simulation was carried out to investigate the failure of a tailings dam triggered by flow liquefaction caused by increased pore pressure in the foundation tailings. The SANISAND constitutive model was employed to capture the undrained brittle behaviour of polymetallic tailings observed in triaxial tests. By utilizing the MPM in Anura3D platform, the SANISAND model effectively simulated the flow liquefaction, and subsequent runout of the tailings released during the dam failure. The simulation results yielded insights into the initiation of flow liquefaction and subsequent large deformations of the tailings. Overall, the SANISAND and MPM/Anura3D combination demonstrated its effectiveness in assessing the behaviour of tailings materials in the event of a dam failure. This mechanics-based simulation approach provides valuable insights into initiating flow liquefaction and subsequent large deformations, which can inform tailings dam design, construction, and risk management.

6 ACKNOWLEDGEMENTS

The authors gratefully acknowledge the financial support by NSERC, Mitacs, and SRK Consulting, which was essential to the completion of this research.

7 REFERENCES

Al-Kafaji I.K. 2013. *Formulation of a dynamic material point method (MPM) for geomechanical problems*. Ph.D. Thesis, University of Stuttgart.

Anura3D MPM Research Community (2021). *Anura3D Version 2021 Source Code*, <www.anura3d.com>.

Barrero, A.R., Taiebat, M., Dafalias, Y.F. 2020. Modeling cyclic shearing of sands in the semifluidized state. *Int. J. Numer. Anal. Meth. Geomech.* 44(3), 371-388.

Castro, G. 1969. *Liquefaction of sands*. Ph.D. Thesis, Harvard University.

Ceccato, F. 2015. *Study of large deformation geomechanical problems with the material point method*. PhD Thesis, Universita Degli Studi Di Padova.

Ceccato, F., Beuth, L., Simonini, P. 2016. Analysis of piezocone penetration under different drainage conditions with the two-phase material point method. *J. Geotech. Geoenviron. Eng.*, **142**(12), 04016066.

Cuomo, S., Ghasemi, S., Martinelli, M., Calvello, M. 2019. Simulation of liquefaction and retrogressive slope failure in loose coarse-grained material. *Int. J. Geomech.*, **19**(10), 04019116.

Dafalias, Y.F., Manzari, M.T. 2004. Simple plasticity sand model accounting for fabric change effects. *J. Engg. Mech.*, **130**(6), 622-634.

Dafalias, Y.F., Taiebat, M. 2016. SANISAND-Z: zero elastic range sand plasticity model. Géotechnique **66**(12), 999-1013.

Davies, M., Chin, B., Dawson, B. 1998. Static liquefaction slump of mine tailings - A case history. *51st Canadian geotechnical conference*. Pages 123-132.

Detournay, C., Dzik, E. 2006. Nodal mixed discretization for tetrahedral elements. *In 4th International FLAC Symposium on Numerical Modeling in Geomechanics* (Vol. **7**). Itasca Consulting Group, Inc. Minneapolis.

Fern, J., Rohe, A., Soga, K., Alonso, E. 2019. *The material point method for geotechnical engineering: a practical guide*. CRC Press.

Fern, E.J., Soga, K. 2016. The role of constitutive models in MPM simulations of granular column collapses. *Acta Geotechnica*, **11**(3), pp.659-678.

Ishihara, K. 1993. Liquefaction and flow failure during earthquakes. *Géotechnique*, **43**(3), 351-451.

Kumar, K. *Multi-scale multiphase modelling of granular flows*. 2014. PhD Thesis, University of Cambridge.

Leong, W., Chu, J., Teh, C. 2000. Liquefaction and instability of a granular fill material. *Geotech. Test. J.*, **23**(2), 178-192.

Lino Ramírez, E.A. 2021. *Modeling of flow liquefaction and large deformations in tailings dams using material point method*. Master Thesis, University of British Columbia.

Macedo, J., Vergaray, L. 2022. Properties of mine tailings for static liquefaction assessment. *Can.Geotech. J.*, **59**(5), 667-687.

Manzari M.T., Dafalias Y.F. 1997. A critical state two-surface plasticity model for sands. *Géotechnique*, **47**(2), 255-72.

Morgenstern, N.R., Vick, S.G., Viotti, C.B., Watts, B.D. 2016. *Report on the immediate causes of the failure of the Fundão dam*. Fundão Tailings Dam Review Panel.

Petalas, A.L., Dafalias, Y.F., Papadimitriou, A.G. 2020 SANISAND-F, Sand constitutive model with evolving fabric anisotropy, *Int. J. Solids Struct.,* 188, 12-31.

Riveros, G.A., Sadrekarimi, A. 2021. Static liquefaction behaviour of gold mine tailings. *Can. Geotech. J.*, **58**(6), 889-901

Robertson, P.K., de Melo, L., Williams, D.J., Wilson, G.W. 2019. *Report of the Expert Panel on the Technical Causes of the Failure of Feijão dam I*.

Schnaid, F., Bedin, J., Viana da Fonseca, A.J.P., de Moura Costa Filho, L. 2013. Stiffness and strength governing the static liquefaction of tailings. *J. Geotech. Geoenviron. Eng.*, **139**(12), 2136-2144.

Soga, K., Alonso, E., Yerro, A., Kumar, K., Bandara, S. 2016. Trends in large-deformation analysis of landslide mass movements with particular emphasis on the material point method. *Géotechnique*, **66**(3), 248-273.

Taiebat, M., Dafalias, Y.F. 2008. SANISAND: Simple anisotropic sand plasticity model. *Int. J. Numer. Anal. Meth. Geomech.*, **32**(8), 915-948.

Taiebat, M., Jeremić, B., Dafalias, Y.F., Kaynia, A.M., Cheng, Z. 2010. Propagation of seismic waves through liquefied soils. *Soil Dyn. Earthquake Eng.,* **30**(4), 236-257.

Yang, M., Taiebat, M., Dafalias, Y.F. 2022 SANISAND-MSf: a sand plasticity model with memory surface and semifluidised state, *Géotechnique*, **72**(3), 227-246.

Yerro, A. *MPM modelling of landslides in brittle and unsaturated soils*. 2015. PhD Thesis, Universitat Politecnica de Catalunya.